CHEMICAL PHYSICS

Observation of the geometric phase effect in the H + HD → H_2 + D reaction

Daofu Yuan[1]*, Yafu Guan[2]*, Wentao Chen[1], Hailin Zhao[2], Shengrui Yu[3], Chang Luo[1], Yuxin Tan[1], Ting Xie[1], Xingan Wang[1]†, Zhigang Sun[2]†, Dong H. Zhang[2]†, Xueming Yang[2,4]†

Theory has established the importance of geometric phase (GP) effects in the adiabatic dynamics of molecular systems with a conical intersection connecting the ground- and excited-state potential energy surfaces, but direct observation of their manifestation in chemical reactions remains a major challenge. Here, we report a high-resolution crossed molecular beams study of the H + HD → H_2 + D reaction at a collision energy slightly above the conical intersection. Velocity map ion imaging revealed fast angular oscillations in product quantum state–resolved differential cross sections in the forward scattering direction for H_2 products at specific rovibrational levels. The experimental results agree with adiabatic quantum dynamical calculations only when the GP effect is included.

In a system of potential energy surfaces (PESs) connected through a conical intersection (CI), a geometric phase (GP) must be introduced that pertains to adiabatic motions encircling the CI for the system to be treated properly in the adiabatic quantum mechanical framework. The GP effect was discovered independently by Pancharatnam in 1956 in crystal optics (*1*) and by Longuet-Higgins *et al.* in 1958 in molecular systems (*2*). In 1984, Berry (*3*) generalized the GP (also known as Berry phase) effect to all adiabatic processes, after which it became a widely studied topic in physics. Over the past three decades, the potentially profound influence of the GP on material properties such as polarization, orbital magnetism, piezoelectric and ferroelectric properties, and quantum Hall effects has become clear (*4*–*6*). The concept of GP is now essential for a coherent understanding of many basic phenomena in physics.

CIs appear in the PESs of many molecular systems and chemical reaction coordinates (*7*). Near a CI, electronic motion and nuclear motion are strongly coupled in contravention of the Born-Oppenheimer approximation. When a molecular system with a CI is treated theoretically in the adiabatic framework, i.e., only considering the lower energy electronic surface, the GP must be introduced to ensure, in accord with quantum mechanics, that the total wave function is single-valued at each nuclear geometry. GP effects have been investigated in detail in isolated molecules such as the sodium trimer (*8*), as well as in the phenol photodissociation process (*9*, *10*).

The most important chemical reaction for the study of the GP effect is the hydrogen exchange reaction, H + H_2 → H_2 + H, because it has a well-defined CI and can be treated most accurately by theory. In the associated set of PESs for this reaction, the CI between the ground electronic state and the first excited state lies at about 2.75 eV (in total energy) (*11*), at which three hydrogen nuclei form an equilateral triangular geometry of D_{3h} symmetry. In pioneering work on the role of GP in the H + H_2 → H_2 + H reaction, Mead and Truhlar showed that the GP would affect observables only if the nuclear wave function encircled the CI, and the effect could be included by introducing a vector potential (*12*). In 1988, Zhang and Miller performed full-dimensional quantum dynamics calculations on the hydrogen exchange reaction without considering the GP effect, which agreed with the relevant experimental observation, suggesting the GP effect is not important in this reaction at low collision energy (*13*, *14*). Kuppermann and co-workers studied the GP effect on the H + H_2 reaction using the multivalued basis functions approach (*15*, *16*) and predicted strong GP effects in the differential cross sections (DCSs). Their predictions, however, were not reproduced by later dynamics calculations (*17*–*19*) and by experiments (*20*, *21*). Quantum reactive scattering studies by Kendrick and co-workers and by Althorpe and co-workers established that the GP effect should be negligible at total energy below 1.8 eV (*19*, *22*–*25*), becoming significant only at total energy above 3.5 eV. Theoretical studies also pointed out that a clear signature of the GP effect on this reaction would be a shift of the fast angular oscillation in DCSs in the sideways scattering direction (*19*, *26*).

Over the past two decades, high-resolution crossed beam studies using the H atom tagging method have probed many important elementary reactions (*27*–*30*), including the H + D_2 and H + HD reactions at various collision energies (*20*, *21*, *31*–*33*). No fast angular oscillations in DCSs for these latter reactions have been observed, most likely because the angular resolution

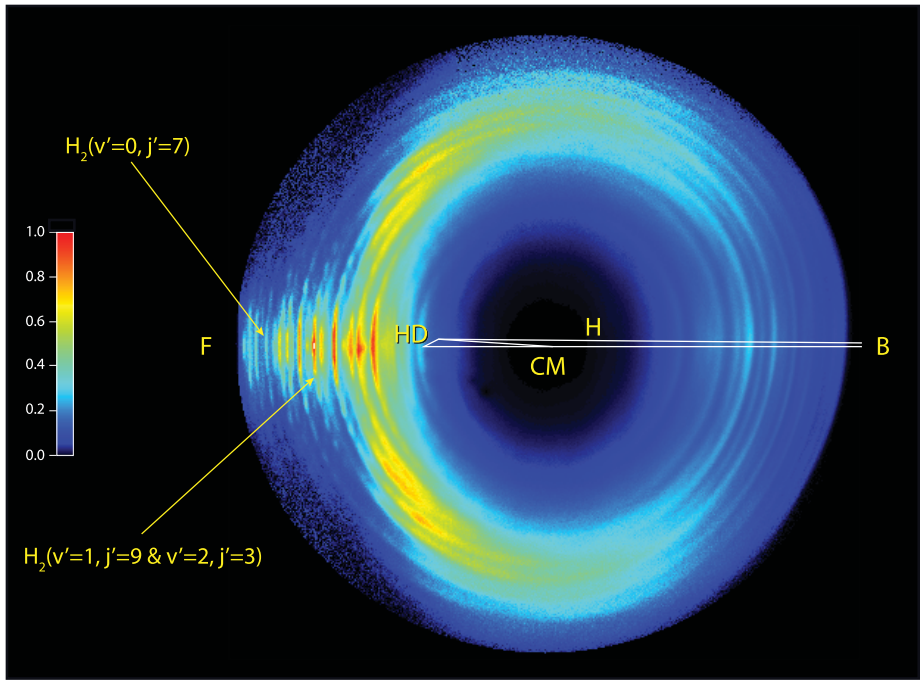

Fig. 1. Experimental images of the D atom product from the H + HD → H_2 + D reaction at a collision energy of 2.77 eV. The crossing angle of the two beams is 160°. F and B denote the forward (0°) and the backward scattering direction (180°) for the H_2 coproduct in the center-of-mass frame (CM) relative to the H atom beam direction, respectively.

[1]Hefei National Laboratory for Physical Sciences at the Microscale and Department of Chemical Physics, University of Science and Technology of China, Hefei, 230026, China. [2]State Key Laboratory of Molecular Reaction Dynamics, Dalian Institute of Chemical Physics, Chinese Academy of Sciences, Dalian, 116023, China. [3]Hangzhou Institute of Advanced Studies, Zhejiang Normal University, Hangzhou, 311231, China. [4]Department of Chemistry, School of Science, Southern University of Science and Technology, Shenzhen, 518055, China.
*These authors contributed equally to this work.
†Corresponding author. Email: xawang@ustc.edu.cn (X.W.); zsun@dicp.ac.cn (Z.S.); zhangdh@dicp.ac.cn (D.H.Z.); xmyang@dicp.ac.cn or yangxm@sustc.edu.cn (X.Y.)

of the experimental method was limited. More recently, the PHOTOLOC (photoinitiated reaction analyzed by the law of cosines) technique has been applied to this search but with a similarly negative outcome (*34*–*36*).

We have developed a high-resolution time-sliced velocity map ion imaging (VMI) apparatus for H(D) atom product detection using the threshold ionization technique for crossed beams scattering studies (*37*). The VMI technique has proven to be a powerful technique for accurately measuring angular distributions of scattering products (*38*). The application of the threshold ionization scheme in this apparatus for D atom product detection in the H + HD → H_2 + D reaction substantially reduced the recoil of the electrons and consequently improved the velocity resolution for the D atom product significantly. Because of the high angular and velocity resolution, fast forward angular oscillations in this reaction at the collision energy of 1.35 eV have been observed and were attributed to corona scatterings in the reaction (*37*). At this collision energy, the reaction appears to occur with a simple direct abstraction mechanism. Through this study, we concluded that the GP effect plays a negligible role in the dynamics of this reaction at this collision energy, which is far below the CI total energy of 2.75 eV (2.53 eV in collision energy).

Here, we report a high-resolution crossed beams study on the H + HD → H_2 + D reaction at a collision energy of 2.77 eV, corresponding to 2.99 eV in total energy relative to the equilibrium energy of an H_2 molecule, or 0.24 eV above the CI. In addition, we have carried out accurate adiabatic quantum mechanical calculations with and without considering the GP effect, as well as diabatic quantum dynamics calculations, to investigate the GP effect on this reaction.

In this experiment, the H atom beam was generated by 193-nm laser photolysis of HI molecules in a pure HI beam at the nozzle tip. The fast H atom beam produced from the H + I($^2P_{3/2}$) channel was selected to react with HD. The HD beam was produced by supersonic expansion through a second pulsed valve (Even Lavie valve). The HD gas sample was cooled to liquid nitrogen temperature before expanding to the source chamber vacuum by means of a pulsed nozzle. About 97% of the HD molecules in the beam were in the ground vibrational and rotational level (v = 0, j = 0). Both the pulsed H atom beam and the HD beam were collimated by skimmers before entering the scattering chamber. The two beams were spatially and temporally overlapped. Differential pumping was used to reduce the residual HI background in the scattering chamber. The D atom product was ionized by means of a two-color [vacuum ultraviolet (VUV) + ultraviolet] threshold ionization scheme and subsequently detected using a VMI detector. During the experiment, the VUV laser wavelength was scanned back and forth to cover the entire Doppler profile of the D atom product to achieve uniform detection efficiency for the D atom products with different velocities. For more details about the experimental setup, refer to the materials and methods in the supplementary materials (SM).

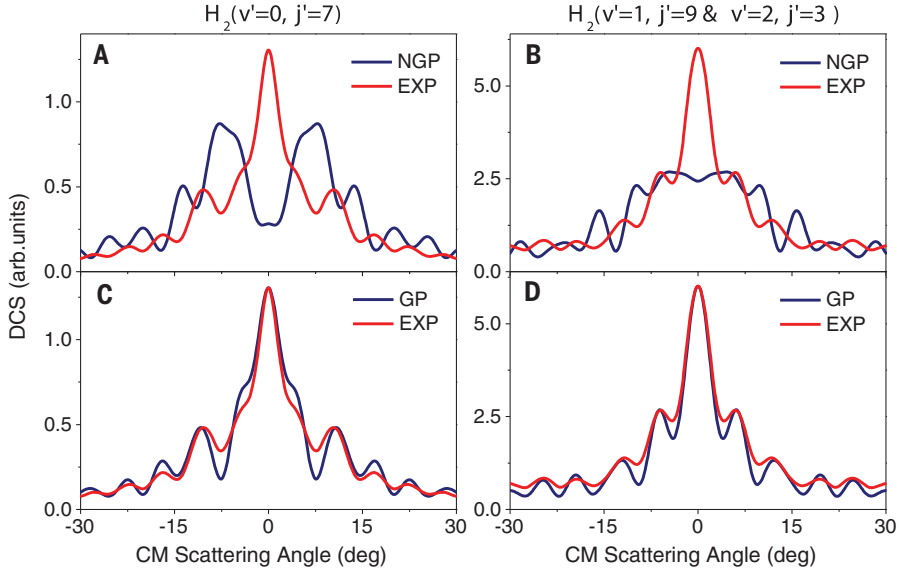

Fig. 2. Comparisons of the experimental (EXP) and theoretical product angular distributions of the H_2 product from the H + HD (v = 0, j = 0) ⟶ H_2 + D reaction at a collision energy of 2.77 eV. (**A** and **C**) Product rovibrational state is v' = 0, j' = 7. (**B** and **D**) Product rovibrational states are v' = 1, j' = 9 and v' = 2, j' = 3, which appear in the measured image as a merged ring. The theoretical results (dark blue lines) do not include the GP (NGP) in panels A and B but do include it (GP) in panels C and D. arb., arbitrary; deg, degree.

The experimental velocity map image of the D atom product from the H + HD → H_2 + D reaction at the collision energy of 2.77 eV (Fig. 1) shows rings that are well resolved in the forward scattering direction. These ring structures correspond to different rovibrational state structures of the H_2 product and are assignable (see fig. S4). Certain ring structures arise from a single rovibrational state, whereas most encompass combined rovibrational states of H_2. For each ring, there are fine oscillations in the angular distribution in the forward direction as observed in the study at the collision energy of 1.35 eV. We then acquired the experimental angular distributions for the H_2 product at the rovibrational level (v' = 0, j' = 7) and at the combined levels (v' = 1, j' = 9 and v' = 2, j' = 3) in the forward scattering direction by extracting the signals at a set of different scattering angles (in 1° intervals) for the corresponding rings (Fig. 2, A and B).

To ascertain whether the GP effect markedly influenced this reaction at this high collision energy, we first carried out adiabatic quantum dynamics calculations on the accurate adiabatic Boothroyd-Keogh-Martin-Peterson-2 (BKMP2) PES with the GP effect not included (Fig. 2, A and B). The angular distribution patterns from the calculations with no GP (NGP) are not in agreement with the corresponding experimental results: The oscillation patterns in the calculated NGP DCS are almost completely out of phase with the experimental results, with theoretical peaks located at the experimental valley positions. In particular, the experimental angular distribution for the H_2 (v' = 0, j' = 7) product state shows a pronounced peak in the exact forward direction (0°), whereas the theoretically calculated NGP distribution exhibits a deep valley there. The same calculations have also been performed on the complete configuration interaction (CCI) PES, which is considered the most accurate adiabatic PES for the reaction system (*39*). The calculated results on the CCI PES are essentially the same as those obtained on the BKMP2 PES (see fig. S5), indicating that the disagreement between the experiment and the NGP calculation is not due to inaccuracies associated with a particular adiabatic PES. Similar comparisons were made for additional H_2 product rovibrational states (see fig. S6), and the NGP-calculated angular distributions similarly disagreed with the experimental results.

We then carried out time-dependent adiabatic quantum dynamics calculations for the reaction on the BKMP2 PES with inclusion of the GP as a vector potential, as Althorpe and co-workers had done for the H + H_2 reaction (*23*). The application of the vector potential for the H + HD reaction is slightly more complicated than for the H + H_2 reaction because of the asymmetric masses. In the present calculations, this vector potential was first derived in the mass-scaled hyperspherical coordinates and then was expressed in the reactant Jacobi coordinates for the subsequent quantum reactive scattering calculations. For more details about the reactive scattering theory including the GP in reactant Jacobi coordinates (*40*), refer to section VI in the SM. The calculated angular distributions with the GP effect included are shown in Fig. 2, C and D. In marked contrast to the NGP results,

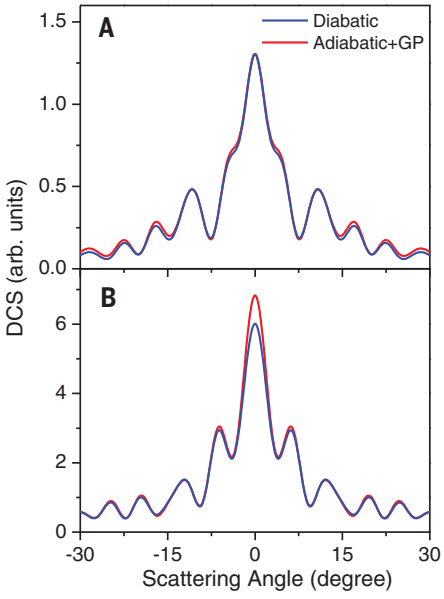

Fig. 3. Comparison between diabatic and adiabatic with GP calculations for H_2 product in specific quantum states. (**A**) H_2 (v' = 0, j' = 7); (**B**) H_2 (v' = 1, j' = 9 and v' = 2, j' = 3).

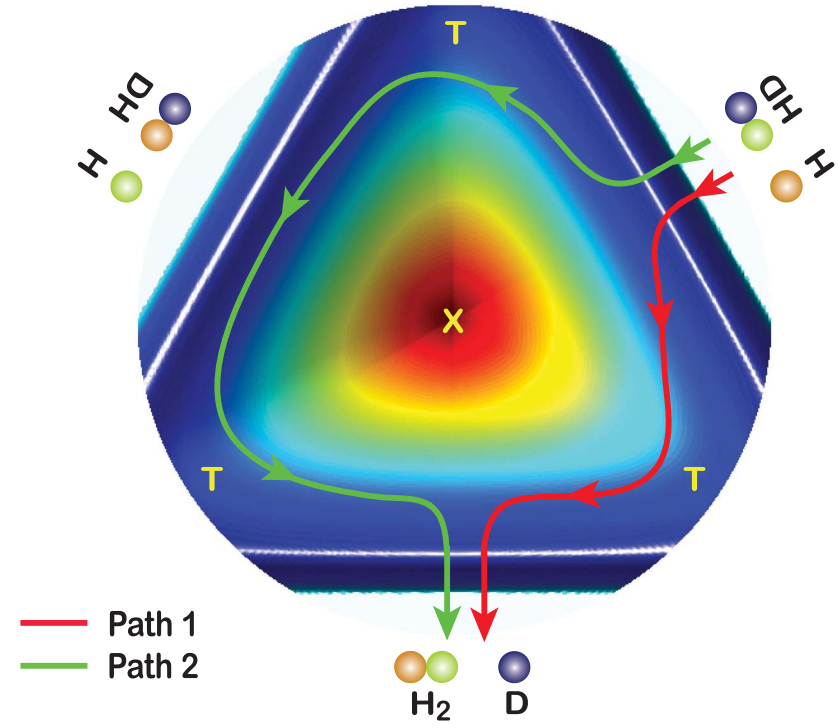

Fig. 4. A cut view through the H + HD PES. The positions of the three H + HD geometric arrangements, transition states (T), and CI (×) are shown. On the surface, representative one–transition state (path 1) and two–transition state (path 2) reaction paths are shown. The cut was calculated using hyperspherical coordinates (*45*) at a given overall separation ρ of 3.60 bohr without consideration of the mass difference between H and D atoms.

the theoretical angular distributions obtained with the GP effect included agree well with the experimental results, with the calculated angular oscillations exactly in phase with the experimental results. This agreement suggests strongly that the GP effect can be seen in the adiabatic picture for this benchmark reaction at this high collision energy. Similar comparisons were made for additional H_2 product levels (fig. S6), and results were consistent with the above conclusion.

Because the collision energy of this experiment is 0.24 eV above the CI, the question arises whether the adiabatic excited state (or the upper cone of the CI) has a significant effect on the reaction dynamics. We therefore developed accurate diabatic PESs for the H_3 system and used them to carry out state-to-state quantum dynamics calculations. To construct the diabatic PESs, we obtained the derivative coupling between the two lowest $^2A'$ states by performing MR-CISD (multireference configuration interaction, with all single and double excitations) calculations using the COLUMBUS program (*41*) with active space comprising three electrons distributed in nine a' and two a'' orbitals and basis of standard aug-cc-pVQZ (*42*). The derivative couplings were then fitted using an artificial neural network method (*43*). The ground adiabatic PES of H_3 was taken as the well-known BKMP2 PES, but the energy difference between the ground and excited states was calculated using the MOLPRO package (*44*) and fitted using the artificial neural network method. See the SM for more details. The DCSs for the title reaction were then calculated using the diabatic PESs for the products H_2 (v' = 0, j' = 7) and H_2 (v' = 1, j' = 9 and v' = 2, j' = 3) and are compared with the corresponding adiabatic GP results in Fig. 3. The calculated DCS using the adiabatic ground-state PES including the GP effect agrees well with the DCS calculated using the diabatic coupled PESs, and the calculated diabatic DCS is also in good agreement with the experimental result, demonstrating that the dynamics of the reaction can be accurately described using the diabatic theory without considering the GP effect, as expected. Therefore, the GP effect associated with the CI in a molecular system exists only in the adiabatic picture. The present results also verify that the adiabatic theory including the GP can be used to describe the detailed dynamics of this chemical reaction at this collision energy as precisely as the diabatic theory does. This, we believe, has important implications for dynamics studies of complicated quantum systems with CIs using adiabatic theory when diabatic treatment is very difficult or not possible.

There are some small differences in the forward scattering peak between the diabatic and the adiabatic GP results for the H_2 product (v' = 1, j' = 9 and v' = 2, j' = 3) (Fig. 3B), implying that the excited state might play some small role at this collision energy. To assess quantitatively the effect of the excited state, we have calculated the time-dependent population of the adiabatic ground (V_1) and excited (V_2) states for H + HD at the collision energy of 2.77 eV for differential partial waves J = 0, 10, 20, 30, and 40. The calculated results show that the J = 0 population on the adiabatic excited state V_2 reaches its maximum at ~46 fs, which is still less than 0.09% of that on the adiabatic ground state (see fig. S7A). In addition, we have also computed the time-independent wave function as a function of hyperradius ρ in hyperspherical coordinates for J = 0 with the two hyperangular coordinates integrated out (*45*). The results show that the wave function of the adiabatic excited V_2 is distributed in a very narrow region around the CI, with peak value less than 1% of that on the adiabatic ground state V_1 (see fig. S7B). By integrating the $|\psi|^2$ distribution in fig. S7B, we estimated that the population on the excited state is only about 0.053% of that on the ground state for the J = 0 partial wave. For partial waves with larger J value, the excited-state contribution becomes even smaller. The excited-state dynamics are different from those on the ground state, thus likely causing the small difference between the adiabatic + GP and the diabatic calculations. These quantitative analyses confirm that the excited state plays a very minor role in the H + HD → H_2 + D reaction at the collision energy of 2.77 eV, suggesting the reaction process occurs predominantly on the ground state and thus ensuring that the reaction at this collision energy can be adequately treated using adiabatic calculations on the ground state PES with GP.

It is intriguing that the GP effect on the H + HD → H_2 + D reaction can be seen so clearly in the forward scattering direction. According to the topological argument proposed by Althorpe and co-workers (*19*, *23*) for the H + H_2 reaction,

the GP effect should not be important for a reaction that occurs through a single pathway, because the GP only introduces a constant phase change to the wave functions of the pathway and thus will not influence the dynamics. In that context, there should be a second reaction pathway at this high collision energy that is markedly different from the normal reaction pathway. Using the topological argument, the GP effect can then change the DCS through interference between the two reaction pathways. By quasi-classical trajectory analysis, Althorpe and co-workers posited that one of the two pathways of the reaction proceeds through a single transition state (path 1), whereas the other proceeds through two transition states (path 2) (*19*). In the case of H + HD → H_2 + D, the GP effect is expected to manifest through the same interference between the two analogous reaction pathways (Fig. 4), and such an effect is more pronounced in the forward scattering direction of certain specific product quantum states at this collision energy.

Althorpe and co-workers also developed an approach to extract the contributions of the two reaction pathways on the basis of the topological argument (*19*, *23*, *24*, *26*). In this approach, the nuclear wave functions for path 1 and path 2 can be calculated by $\psi_1 = (\psi_{NGP} + \psi_{GP})/\sqrt{2}$ and $\psi_2 = (\psi_{NGP} - \psi_{GP})/\sqrt{2}$, respectively, where ψ_{NGP} and ψ_{GP} are the calculated wave functions without and with the GP effect, respectively. The scattering amplitudes from path 1 and path 2 can be expressed as $f_1(\theta) = [f_{NGP}(\theta) + f_{GP}(\theta)]/\sqrt{2}$ and $f_2(\theta) = [f_{NGP}(\theta) - f_{GP}(\theta)]/\sqrt{2}$, respectively. The square moduli of $f_1(\theta)$ and $f_2(\theta)$, $|f_1(\theta)|^2$ and $|f_2(\theta)|^2$, give the angular distributions of the product, i.e., the DCSs, for the individual paths. The total product DCS for the whole reaction can be described as

$$\sigma(\theta) = |f_1(\theta) + f_2(\theta)|^2 = |f_1(\theta)|^2 + |f_2(\theta)|^2 + f_1^*(\theta)f_2(\theta) + f_1(\theta)f_2^*(\theta)$$

whereas the interference between two pathways comes from the last two crossing terms. If the GPs introduced are different for the two pathways, then a difference in the DCS ensues. This explains the GP effect in the present case. The integral cross sections (ICSs) for the reaction via path 1 and path 2 can thus be calculated by integrating the corresponding DCS for all reaction product states.

Using this approach, we computed the total ICS for the reaction via path 1 and path 2 for collision energy up to 4 eV (Fig. 5A). At collision energies below 1.5 eV, the H + HD → H_2 + D reaction proceeds almost completely through path 1, which is the typical abstraction reaction pathway. As a result, the interference between products from path 1 and path 2 is negligible at low collision energy, and thus, the GP does not influence the dynamics of the reaction. However, as shown in Fig. 5A, at collision energies above 1.5 eV, the contribution from path 2 becomes increasingly important as the collision energy increases, even though the overall contribution from path 2 is still small at the collision energy

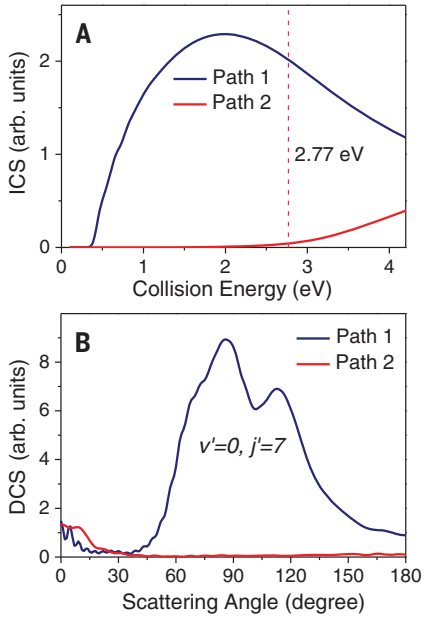

Fig. 5. Relative ICSs and DCSs from path 1 and path 2. (**A**) Calculated reactive ICSs as a function of collision energy for the H + HD ⟶ H_2 + D reaction proceeding through either path 1 or path 2; the ICS of path 2 is only 2.3% of that of path 1 at a collision energy of 2.77 eV. (**B**) Calculated DCS for the H_2 (v' = 0, j' = 7) product at a collision energy of 2.77 eV from path 1 and path 2. In the forward scattering direction, the DCSs from path 1 and 2 have comparable amplitudes, thus causing strong interference between the two paths.

of 2.77 eV, accounting for only ~2.3% of the total product.

To explore why the GP effect is so pronounced in the forward scattering direction, we calculated the DCS for the H_2 (v' = 0, j' = 7) product from path 1 and path 2 at the collision energy of 2.77 eV. The calculations show that the two reaction paths exhibit very different angular distributions (Fig. 5B), as in the H + H_2 reaction (*23*). Path 1 leads to predominantly sideways-scattered products with relatively small amplitude in the forward and backward scattering directions, whereas path 2 leads mainly to forward scattering. Coincidentally, the forward scattering amplitude for the two paths of this reaction are comparable (see Fig. 5B). With different phases introduced by the GP effect to the two paths, their comparable scattering amplitudes make the GP effect more pronounced in the forward scattering direction. In the backward and sideways scattering direction, it would be much harder to see the GP effect because of the dominance of path 1 over path 2. The detailed mechanism of path 2 through two transition states should be very similar to that of the H + H_2 → H_2 + H reaction (*46*). Here, we want to emphasize that the GP is introduced theoretically for accurate treatment of the molecular system in the adiabatic picture; thus, the GP effect on the dynamics and its observation should be discussed strictly in the context of the adiabatic theory.

This work demonstrates that fine angularly resolved scattering structure in the forward direction for reaction products in specific quantum states is an extremely sensitive probe of the GP effect in quantum dynamics of chemical reactions in the adiabatic picture.

REFERENCES AND NOTES

1. S. Pancharatnam, *Proc. Indian Acad. Sci. A* **44**, 247–262 (1956).
2. H. C. Longuet-Higgins, U. Öpik, M. H. L. Pryce, R. A. Sack, *Proc. R. Soc. London Ser. A* **244**, 1–16 (1958).
3. M. V. Berry, *Proc. R. Soc. London Ser. A* **392**, 45–57 (1984).
4. D. Xiao, M. C. Chang, Q. Niu, *Rev. Mod. Phys.* **82**, 1959–2007 (2010).
5. N. Nagaosa, J. Sinova, S. Onoda, A. H. MacDonald, N. P. Ong, *Rev. Mod. Phys.* **82**, 1539–1592 (2010).
6. J. Sinova, S. O. Valenzuela, J. Wunderlich, C. H. Back, T. Jungwirth, *Rev. Mod. Phys.* **87**, 1213–1260 (2015).
7. W. Domcke, D. R. Yarkony, H. Köppel, Eds., *Conical Intersections: Electronic Structure, Dynamics and Spectroscopy* (World Scientific, 2003).
8. H. von Busch *et al.*, *Phys. Rev. Lett.* **81**, 4584–4587 (1998).
9. M. G. D. Nix, A. L. Devine, R. N. Dixon, M. N. R. Ashfold, *Chem. Phys. Lett.* **463**, 305–308 (2008).
10. C. Xie *et al.*, *J. Am. Chem. Soc.* **138**, 7828–7831 (2016).
11. A. J. C. Varandas, F. B. Brown, C. A. Mead, D. G. Truhlar, N. C. Blais, *J. Chem. Phys.* **86**, 6258–6269 (1987).
12. C. A. Mead, D. G. Truhlar, *J. Chem. Phys.* **70**, 2284–2296 (1979).
13. J. Z. H. Zhang, S.-I. Chu, W. H. Miller, *J. Chem. Phys.* **88**, 6233–6239 (1988).
14. J. Z. H. Zhang, W. H. Miller, *Chem. Phys. Lett.* **153**, 465–470 (1988).
15. B. Lepetit, A. Kuppermann, *Chem. Phys. Lett.* **166**, 581–588 (1990).
16. Y.-S. M. Wu, A. Kuppermann, B. Lepetit, *Chem. Phys. Lett.* **186**, 319–328 (1991).
17. M. P. de Miranda, D. C. Clary, J. F. Castillo, D. E. Manolopoulos, *J. Chem. Phys.* **108**, 3142–3153 (1998).
18. B. K. Kendrick, *J. Chem. Phys.* **112**, 5679–5704 (2000).
19. J. C. Juanes-Marcos, S. C. Althorpe, E. Wrede, *Science* **309**, 1227–1230 (2005).
20. E. Wrede, L. Schnieder, *J. Chem. Phys.* **107**, 786–790 (1997).
21. E. Wrede *et al.*, *J. Chem. Phys.* **110**, 9971–9981 (1999).
22. B. Kendrick, *J. Phys. Chem. A* **107**, 6739–6756 (2003).
23. J. C. Juanes-Marcos, S. C. Althorpe, *J. Chem. Phys.* **122**, 204324 (2005).
24. F. Bouakline, S. C. Althorpe, D. Peláez Ruiz, *J. Chem. Phys.* **128**, 124322 (2008).
25. B. K. Kendrick, J. Hazra, N. Balakrishnan, *Phys. Rev. Lett.* **115**, 153201 (2015).
26. S. C. Althorpe, *J. Chem. Phys.* **124**, 084105 (2006).
27. B. R. Strazisar, C. Lin, H. F. Davis, *Science* **290**, 958–961 (2000).
28. M. Qiu *et al.*, *Science* **311**, 1440–1443 (2006).
29. T. Wang *et al.*, *Science* **342**, 1499–1502 (2013).
30. T. Yang *et al.*, *Science* **347**, 60–63 (2015).
31. L. Schnieder, K. Seekamp-Rahn, E. Wrede, K. H. Welge, *J. Chem. Phys.* **107**, 6175–6195 (1997).
32. S. A. Harich *et al.*, *Nature* **419**, 281–284 (2002).
33. D. Dai *et al.*, *Science* **300**, 1730–1734 (2003).
34. J. Jankunas, M. Sneha, R. N. Zare, F. Bouakline, S. C. Althorpe, *J. Chem. Phys.* **139**, 144316 (2013).
35. H. Gao, M. Sneha, F. Bouakline, S. C. Althorpe, R. N. Zare, *J. Phys. Chem. A* **119**, 12036–12042 (2015).
36. W. Hu, G. C. Schatz, *J. Chem. Phys.* **125**, 132301 (2006).
37. D. Yuan *et al.*, *Nat. Chem.* **10**, 653–658 (2018).
38. A. T. J. B. Eppink, D. H. Parker, *Rev. Sci. Instrum.* **68**, 3477–3484 (1997).
39. S. L. Mielke, B. C. Garrett, K. A. Peterson, *J. Chem. Phys.* **116**, 4142–4161 (2002).
40. Z. Sun, H. Guo, D. H. Zhang, *J. Chem. Phys.* **132**, 084112 (2010).
41. H. Lischka *et al.*, *Phys. Chem. Chem. Phys.* **3**, 664–673 (2001).
42. T. H. Dunning Jr., *J. Chem. Phys.* **90**, 1007–1023 (1989).

43. I. E. Lagaris, A. Likas, D. I. Fotiadis, *IEEE Trans. Neural Netw.* **9**, 987–1000 (1998).
44. H. J. Werner *et al*., MOLPRO, version 2012.1. A package of ab initio programs (2012).
45. R. T. Pack, G. A. Parker, *J. Chem. Phys.* **87**, 3888–3921 (1987).
46. F. Bouakline, S. C. Althorpe, P. Larregaray, L. Bonnet, *Mol. Phys.* **108**, 969–980 (2010).

ACKNOWLEDGMENTS

We thank J. Sang and S. Wang for their help with the experiments. **Funding:** This work was supported by National Natural Science Foundation of China (no. 21688102, no. 21127902, no. 21433009), Chinese Academy of Sciences (grant no. XDB 17010000), and Ministry of Science and Technology. **Author contributions:** D.Y., W.C., C.L., Y.T., T.X., X.W., and X.Y. performed the crossed beams experiments and data analysis. Y.G., H.Z., Z.S., and D.H.Z. performed the quantum dynamics calculations and data analysis. X.W., Z.S., D.H.Z., and X.Y. designed the research. X.W., Z.S., D.H.Z., and X.Y. wrote the manuscript. **Competing interests:** The authors declare no competing interests. **Data and materials availability:** All data are available in the supplementary data file.

SUPPLEMENTARY MATERIALS

www.sciencemag.org/content/362/6420/1289/suppl/DC1
Materials and Methods
Supplementary Text
Figs. S1 to S9
Tables S1 and S2
References (*47*–*55*)
Data S1

18 August 2018; accepted 2 November 2018
10.1126/science.aav1356

Science

Observation of the geometric phase effect in the H + HD → H_2 + D reaction

Daofu Yuan, Yafu Guan, Wentao Chen, Hailin Zhao, Shengrui Yu, Chang Luo, Yuxin Tan, Ting Xie, Xingan Wang, Zhigang Sun, Dong H. Zhang and Xueming Yang

Science **362** (6420), 1289-1293.
DOI: 10.1126/science.aav1356

Pinpointing the role of geometric phase

During chemical reactions, electrons usually rearrange more quickly than nuclei. Thus, theorists often adopt an adiabatic framework that considers vibrational and rotational dynamics within single electronic states. Near the regime where two electronic states intersect, the dynamics get more complicated, and a geometric phase factor is introduced to maintain the simplifying power of the adiabatic treatment. Yuan *et al.* conducted precise experimental measurements that validate this approach. They studied the elementary H + HD reaction at energies just above the intersection of electronic states and observed angular oscillations in the product-state cross sections that are well reproduced by simulations that include the geometric phase.

Science, this issue p. 1289